Analytical and Numerical Study of Electron Velocity Distribution Function in a Hall Discharge

IEPC-2017-086

Presented at the 35th International Electric Propulsion Conference
Georgia Institute of Technology • Atlanta, Georgia • USA
October 8 – 12, 2017

Andrey Shagayda[1], Aleksey Tarasov[2], and Dmitry Tomilin[3]
SSC FSUE Keldysh Research Centre, Moscow, Russian Federation

Abstract: The electron velocity distribution function in the low-pressure discharges with the crossed electric and magnetic fields, which occur in magnetrons, plasma accelerators and Hall thrusters with closed electron drift, is not Maxwellian. A deviation from equilibrium is caused by a large electron mean free path relative to the Larmor radius and the size of the discharge channel. In this study, we derived in the relaxation approximation the analytical expression of the electron velocity distribution function in a weakly ionized Lorentz plasma with the crossed electric and magnetic fields in the presence of the electron density and temperature gradients in the direction of the electric field. The solution is obtained in the stationary approximation far from boundary surfaces, when diffusion and mobility are determined by the classical effective collision frequency of electrons with ions and atoms. The moments of the distribution function including the average velocity, the stress tensor, and the heat flux were calculated and compared with the classical hydrodynamic expressions. A theoretical study is presented of the electrostatic electron cyclotron instability involving Bernstein modes for the obtained distribution function in the spatially uniform plasma. Particle-in-cell simulations were used to study the nonlinear evolution of the instability.

Nomenclature

A_n, A_T	=	expressions in the distribution function formula
b	=	subscript related to the electron “birth” distribution function
$\mathbf{B}$	=	magnetic field
$\mathbf{c}$	=	electron velocity in a reference frame moving at a drift velocity
e	=	elementary charge
$\mathbf{E}$	=	electric field
E_T	=	characteristic thermal electric field
F	=	dimensionless electron velocity distribution function
f , f_b	=	electron velocity distribution function and electron birth distribution function respectively
I_k	=	modified Bessel function of the first kind of order k
J_k	=	Bessel function of the first kind of order k
L	=	space domain length in the simulation model
m	=	electron mass

[1] Leading Researcher, Department of Electrophysics, shagayda@gmail.com.
[2] Senior Researcher, Department of Electrophysics.
[3] Leading Researcher, Department of Electrophysics.

n	=	electron number density
P_{ij}	=	stress tensor component
p	=	pressure
$\mathbf{q}$	=	heat flux
$\mathbf{r}$	=	radius vector
S	=	collision term
T	=	temperature
t	=	time
$\mathbf{u}$	=	dimensionless electron velocity in a reference frame moving with the drift velocity
$\mathbf{V}$	=	average electron flow velocity
V_{Tb}	=	average electrons thermal velocity, which they acquire after the collision
$\mathbf{v}$	=	dimensionless electron velocity
$\mathbf{W}$	=	electron drift velocity in the crossed electric and magnetic fields
$\mathbf{w}$	=	dimensionless electron drift velocity in the crossed electric and magnetic fields
α	=	parameter of the "thermal ring" distribution function
α_{ij}	=	coefficients in the stress tensor formula
β	=	parameter reciprocal of the Hall parameter
γ_{ij}	=	coefficients in the stress tensor formula
$\Delta_c, \Delta_V, \Delta_q$	=	kinetic corrections to the transport equations
δ_{ij}	=	Kronecker delta
ε_0	=	permittivity of free space
ε_D	=	characteristic electron drift energy
ε_E	=	wave electric field energy
ε_i	=	ionization energy
ε_T	=	characteristic energy of the electron thermal motion
$\langle \varepsilon_x \rangle$	=	average electron energy loss in the excitation collisions
ζ	=	dimensionless coordinate z
η_{ij}	=	coefficients in the stress tensor formula
λ_D	=	Debye length
ν	=	effective collision frequency
$\nu_q, \nu_e, \nu_x, \nu_i$	=	Coulomb, elastic, excitation and ionization collision frequencies respectively
$\boldsymbol{\xi}$	=	electron velocity
χ	=	auxiliary phase angle characterizing the position of an electron on a cycloid
ψ	=	phase angle characterizing the position of an electron on a cycloid
ω_c	=	electron cyclotron frequency
ω_p	=	electron plasma frequency

I. Introduction

THE study of weakly ionized plasma in the crossed electric and magnetic fields is of great importance for the simulation of magnetrons, plasma accelerators and Hall thrusters[1,2]. In these devices, the discharge is maintained by applying a constant potential difference between the anode and the cathode. The external constant magnetic field has a direction predominantly perpendicular to the electric field. The electrons drift in the crossed fields and ionize the neutral atoms. The ions are accelerated under the influence of the applied potential difference and form together with the electrons an electrically neutral plasma stream. The neutral atom density in these devices is kept sufficiently low providing rare ion-atom collisions to effectively accelerate the ions. Due to a low pressure of neutral gas, electron-atom collisions are also rare and the electron Larmor frequency is many times higher than that of collisions of electrons with atoms, ions, and the discharge channel walls. Therefore, the Hall discharge plasma is characterized by high values of the Hall parameter, which is the ratio of the electron Larmor frequency to the momentum transfer collision frequency.

At present, the problem of numerical modeling of plasma dynamics in the Hall discharge has not been completely solved[3]. The main obstacle is the problem of modeling the motion of electrons. The modeling of the electron flow in the kinetic approximation is extremely time consuming. The so-called "hybrid" models, in which the motion of electrons is simulated in the hydrodynamic approximation, and heavy ions and neutral atoms are considered as particles, provide a significant advantage in volume and speed of calculations[4-11]. However, the use of the classical equations of hydrodynamics is justified only in those cases when the distribution function of the simulated particles is close to equilibrium. It takes place either at a high collision frequency or by the availability of some other processes that lead to a rapid relaxation of the distribution function toward equilibrium. A relatively low frequency of the electron momentum transfer collisions and, accordingly, a large electron mean free path compared to the Larmor radius and the size of the discharge channel can cause significant deviations of the electron velocity distribution function (EVDF) from equilibrium.

The electron distribution function in the Hall discharge plasma is usually studied numerically[12,13]. The general approach to the derivation of analytical expressions assumes a small deviation of the EVDF from equilibrium[14-16]. This assumption is not entirely true for the Hall discharge plasma in which the deviation from equilibrium is big and may lead even to the nonmonotonic behavior of the electron energy distribution function[17]. Several studies[18,19] have been devoted to the influence of secondary electron emission from the discharge channel walls on the formation of an anisotropic EVDF. However, anisotropy of the EVDF may occur in the absence of walls too because of the fundamental characteristics of the electron motion in the crossed electric and magnetic fields.

In this work, we do not set the task of reconstructing in detail the form of the distribution function in the Hall type devices. There are many factors influencing on the movement of electrons in a real discharge. These include, for example, the following factors: inhomogeneity of the electric and magnetic field; centrifugal forces in the devices with annular discharge channel; electron diffuse scattering and secondary electron emission on the walls of the discharge channel; longitudinal plasma oscillations and azimuthal waves. Such a complex problem can be solved only by numerical methods. Our goal is to reveal the principal differences between the Maxwellian distribution function and the distribution function in a weakly ionized plasma with crossed electric and magnetic fields where collisions with heavy particles are dominant. Further, to indicate this type of plasma, we will use the term “Hall discharge plasma”.

Earlier we derived an analytical expression of the EVDF for the case of a weakly ionized Lorentz plasma in the spatially uniform approximation[20]. The aim of this paper is to extend the previously obtained results to the case of a non-uniform plasma and calculate the EVDF in the presence of the electron number density and temperature gradients in the direction of the electric field. Since the distribution function may be nonmonotonic at some plasma parameters, we also investigated the electrostatic electron cyclotron instability involving Bernstein modes caused by this distribution. The purpose of this study was to understand if there is any universal form to which the distribution function approaches, if the instability does occur.

The paper is organized as follows. First, the kinetic equation is described and the statement of the problem is formulated in Sec. II. In Sec. III, the kinetic equation is solved and the EVDF is obtained. In Sec. IV, the shape of the EVDF at different conditions of the problem is considered. In Sec. V, the moments of the EVDF are calculated. In Sec. VI, the electrostatic electron cyclotron instabilities are studied theoretically and using 1D2V particle-in-cell simulation model.

II. Formulation of the Problem

A. Kinetic Equation

In a plasma of the Hall type, the number density of neutral atoms is approximately one or two orders of magnitude higher than the number density of charged particles. Typical parameters of such a plasma are considered in detail, for example, in Ref. 21. At characteristic electron energies above 10 eV in such a plasma, the effective frequencies of Coulomb electron-electron and electron-ion collisions are tens of times smaller than the electron-atom collision frequency. For this reason, no rapid maxwellization of electrons occurs in the Hall type plasma. Because of the smallness of the Coulomb electron-electron collisions frequency, electrons rarely exchange energy among themselves, and much more often, the energy of the electrons directed drift is converted into thermal energy because of collisions with heavy slow particles.

Since most of the collisions are not Coulomb ones and scattering not occurs at small angles, in the kinetic numerical models of the Hall discharge the Fokker-Planck equation is not usually used. The exact kinetic Boltzmann equation is also usually not used because it is rather complicated and requires taking into account the differential cross sections for different types of collisions, which are poorly known. Therefore, simplified models are usually used to describe the electron-atom collisions. These models operate with effective collision frequencies, and the most common assumption is the isotropic distribution of the scattered electrons. Such simplifications are, in fact, very close to the basic assumptions on which the Bhatnagar-Gross-Krook (BGK) collision model is based[22].

Our formal set up is as follows. We consider a weakly ionized plasma in the presence of the uniform crossed electric and magnetic fields. The electron diffusion and mobility are determined by the classical effective collision frequency. The density of the gas, the degree of ionization and the strength of the fields are assumed to be such that electron collisions with heavy particles are dominated. Under these conditions, the Boltzmann type kinetic equation for the electrons with the BGK collision term can be written in the form

$$\frac{\partial f}{\partial t}+\boldsymbol{\xi}\frac{\partial f}{\partial \mathbf{r}}-\frac{e}{m}\left(\mathbf{E}+\boldsymbol{\xi}\times\mathbf{B}\right)\frac{\partial f}{\partial \boldsymbol{\xi}}=\nu\left(f_b-f\right), \tag{1}$$

where f is the electron velocity distribution function; $\mathbf{r}$ is the radius vector; $\boldsymbol{\xi}$ is the velocity vector; $\mathbf{E}$ is the electric field; $\mathbf{B}$ is the magnetic induction vector; ν is the effective frequency of collisions; f_b is the so-called electron "birth" distribution function (EBDF) which describes the velocity distribution just after collision. The EBDF is assumed to be locally equilibrium, i.e.

$$f_b=n_b\left(\pi V_{Tb}^2\right)^{-3/2}\exp\left(-\xi^2/V_{Tb}^2\right), \tag{2}$$

where $V_{Tb}=\sqrt{2T_b/m}$ is the average thermal velocity of the electrons, which they acquire after the collision. Since the average velocity of the ions and neutral atoms substantially less than the velocity of the electrons, here it is assumed that the average electron velocity vector after the collision is equal to zero.

When analyzing the non-equilibrium distribution functions, we will use the standard definition of the hydrodynamic macroparameters accepted in the kinetic theory[23]: $n=\int f\,d\boldsymbol{\xi}$ is the electron density; $\mathbf{V}=(1/n)\int f\,\boldsymbol{\xi}\,d\boldsymbol{\xi}$ is the average velocity; $P_{ij}=m\int\left(\xi_i-V_i\right)\left(\xi_j-V_j\right)f\,d\boldsymbol{\xi}$ is the stress tensor; $p=\left(P_{xx}+P_{yy}+P_{zz}\right)/3$ is the pressure; $T_i=P_{ii}/n$ is the *i- th* component of the temperature; $T=p/n$ is the average temperature (all temperatures are expressed in energy units); $\mathbf{q}=(m/2)\int\left(\boldsymbol{\xi}-\mathbf{V}\right)\left(\boldsymbol{\xi}-\mathbf{V}\right)^2 f\,d\boldsymbol{\xi}$ is the heat flux vector.

The most important types of electron collisions in a Hall type discharge are elastic, excitation and ionization collisions with atoms, and Coulomb collisions with ions. Thus, we take the effective collision frequency as the sum $\nu=\nu_q+\nu_e+\nu_x+\nu_i$ of the Coulomb, elastic, excitation and ionization frequencies respectively. To describe these collisions within the BGK model the collision term $S(f)=\nu\left(f_b-f\right)$ must satisfy the following conservation laws:

$$\int S(f)d\boldsymbol{\xi}=\nu_i n;\quad \int\boldsymbol{\xi}S(f)d\boldsymbol{\xi}=-\nu n\mathbf{V};\quad \int\frac{m\xi^2}{2}S(f)d\boldsymbol{\xi}=-\left(\nu_i\varepsilon_i+\nu_x\langle\varepsilon_x\rangle\right)n, \tag{3}$$

where $\langle\varepsilon_x\rangle$ is the average energy loss in the excitation collisions, and ε_i is the ionization energy. The second relationship in Eq. (3) is fulfilled automatically for $S(f)$ under consideration. The first and the third relationships lead to the following equations:

$$n_b=\frac{\nu+\nu_i}{\nu}n; \tag{4}$$

$$\frac{3}{2}T_b = \frac{\nu}{\nu+\nu_i}\left(\frac{3}{2}T + \frac{mV^2}{2}\right) - \frac{\nu_x\langle\varepsilon_x\rangle}{\nu+\nu_i} - \frac{\nu_i\varepsilon_i}{\nu+\nu_i}. \quad (5)$$

Thus, Eqs. (1), (2), (4) and (5) form a closed system of equations to be solved.

Before we go to solving, we will write a set of hydrodynamic equations that follow from the kinetic equation (1). Availability of this set will allow comparing the values of the diffusion rate, mobility, and thermal conductivity calculated in the hydrodynamic and the kinetic approximations.

B. Equations of Moments

After multiplying Eq. (1) by the electron mass m, momentum $m\boldsymbol{\xi}$ and energy $m\xi^2/2$ and integrating over velocities, we obtain the following system of equations

$$\frac{\partial n}{\partial t} + \frac{\partial(nV_j)}{\partial x_j} = \nu_i n \quad (6)$$

$$\frac{\partial V_j}{\partial t} + V_k\frac{\partial V_j}{\partial x_k} + \frac{1}{mn}\frac{\partial P_{jk}}{\partial x_k} + \frac{e}{m}\left(E_j + [\mathbf{V}\times\mathbf{B}]_j\right) = -(\nu+\nu_i)V_j \quad (7)$$

$$\frac{\partial T}{\partial t} + V_j\frac{\partial T}{\partial x_j} + \frac{2}{3n}P_{jk}\frac{\partial V_j}{\partial x_k} + \frac{2}{3n}\frac{\partial q_j}{\partial x_j} = (\nu+\nu_i)\frac{2m}{3}V^2 - \nu_x\frac{2\langle\varepsilon_x\rangle}{3} - \nu_i\left(\frac{m}{3}V^2 + T + \frac{2\varepsilon_i}{3}\right). \quad (8)$$

Let the electric field and the magnetic field be uniform and perpendicular to each other, and the plasma have the electron number density and temperature gradients only in the direction of the electric field. We choose the orthogonal coordinate system, in which the magnetic field is directed along the *x*-axis, and the electric field is directed along the *z*-axis. Taking Eq. (7) for the velocity components lying in a plane perpendicular to the magnetic field and neglecting the convective derivatives dV_y/dz and dV_z/dz in the stationary approximation we obtain:

$$V_z = -\frac{(\nu+\nu_i)}{\omega_c^2 + (\nu+\nu_i)^2}\frac{1}{mn}\left(enE + \frac{dP_{zz}}{dz} + \frac{\omega_c}{(\nu+\nu_i)}\frac{dP_{yz}}{dz}\right), \quad (9)$$

where $\omega_c = eB/m$ is the electron cyclotron frequency.

When studying the Hall type discharge, in Eq. (9) it is usually assumed that $\omega_c^2 >> (\nu+\nu_i)^2$. It is also assumed that the electron temperature is isotropic. It allows simplifying the stress tensor by recording it as the product of the unit tensor on the pressure $P_{jk} = \delta_{jk}nT$. The result is a classic expression for the diffusion rate across the magnetic field

$$V_z = -\frac{(\nu+\nu_i)}{\omega_c^2}\left(\frac{e}{m}E + \frac{1}{mn}\frac{d(nT)}{dz}\right), \quad (10)$$

which is most often used in the hybrid and hydrodynamic models.

Note that although the model collision integral in Eq. (1) includes the total electron collision frequency $\nu = \nu_q + \nu_e + \nu_x + \nu_i$, the expression of the mobility and the diffusion rate (10) includes not this frequency, but the frequency $(\nu+\nu_i)$. Thus, in the hydrodynamic approximation the effective electron collision transport frequency must include the doubled ionization collision frequency. We call attention to this, because in all publications, known to us, the frequency ν was used in the macroscopic transport equations. This inaccuracy does not usually lead to a significant error in the solution of one-dimensional and two-dimensional models, as to account for the anomalous conductivity these models include an additional empirical frequency $\nu_\alpha = K_\alpha \omega_c$, which is more than an order of magnitude greater than the classic collision frequency. In this case the unaccounted additive to the effective transport frequency becomes unnoticeable against the background of the large magnitude of ν_α. However, in the three-dimensional models, as well as in the two-dimensional, in which one of the coordinates is the azimuth direction angle, there is no need to use the anomalous collision frequency, and the mentioned correction may play a significant role.

III. Solution of the Kinetic Equation

To calculate the distribution function, we will use the integral form of the kinetic equation. At a constant collision frequency, away from the boundary surfaces the distribution function, which satisfies the equation (1), may be represented in the form of the integral along the electron trajectory in the phase space[23]

$$f(t,\mathbf{r},\boldsymbol{\xi}) = \nu \int_{-\infty}^{t} f_b(t_1,\mathbf{r}_1,\boldsymbol{\xi}_1) \exp[-\nu(t-t_1)] dt_1 , \tag{11}$$

where $\mathbf{r}_1$ and $\boldsymbol{\xi}_1$ are the coordinate and velocity of the electron at the time $t_1 < t$.

We seek a stationary solution of this equation in the uniform crossed electric and magnetic fields. As in the previous section, we choose an orthogonal coordinate system in which the magnetic field $\mathbf{B}$ and the electric field $\mathbf{E}$ are directed along the *x*-axis and *z*-axis, respectively. Then the phase trajectory is described by a system of equations:

$$\begin{cases} \mathbf{r}_1 = \mathbf{r} - \dfrac{1}{\omega_c} \mathbf{D}_\psi \cdot \mathbf{c} - \dfrac{\psi}{\omega_c} \mathbf{W} \\ \boldsymbol{\xi}_1 = \mathbf{A}_\psi \cdot \mathbf{c} + \mathbf{W} \end{cases} , \tag{12}$$

where $\mathbf{W} = (0,\, E/B,\, 0)$ is the electron drift velocity in the crossed electric and magnetic fields in the absence of collisions, and the following notations are introduced:

$$\mathbf{c} = \boldsymbol{\xi} - \mathbf{W}; \quad \psi = \omega_c(t-t_1); \quad \mathbf{D}_\psi = \begin{pmatrix} \psi & 0 & 0 \\ 0 & \sin\psi & (1-\cos\psi) \\ 0 & -(1-\cos\psi) & \sin\psi \end{pmatrix}; \quad \mathbf{A}_\psi = \begin{pmatrix} 1 & 0 & 0 \\ 0 & \cos\psi & \sin\psi \\ 0 & -\sin\psi & \cos\psi \end{pmatrix}.$$

Substituting the equilibrium EBDF from Eq. (2) into Eq. (11) we get

$$f(\mathbf{r},\boldsymbol{\xi}) = \beta \int_0^\infty n_{b1} \left(\pi V_{Tb1}^2\right)^{-3/2} \exp\left[-\xi_1^2 / V_{Tb1}^2 - \beta\psi\right] d\psi , \tag{13}$$

where $\beta = \nu/\omega_c$ is a reciprocal of the Hall parameter. In this expression, the values of n_{b1} and V_{Tb1} are taken at the point $\mathbf{r}_1$.

If the plasma parameters have gradients only in the direction of the electric field, the improper integral in Eq. (13) can be reduced to the integral over a period of the cyclotron rotation. Really, since the values of n_{b1} and V_{Tb1} depend only on the coordinate z_1, then due to Eq. (12) they are periodic functions of the phase ψ. The velocity vector $\boldsymbol{\xi}_1$ according to Eq. (12) is also a periodic function of ψ and therefore Eq. (13) can be written as follows:

$$f = \beta \int_0^\infty \Phi(\psi) \exp(-\beta\psi) d\psi , \tag{14}$$

where $\Phi(\psi) = n_{b1}\left(\pi V_{Tb1}^2\right)^{-3/2} \exp\left(-\xi_1^2 / V_{Tb1}^2\right)$ is the periodical function of ψ. Rewriting the integral in Eq. (14) as the sum of the integrals over period, we obtain

$$f = \beta \sum_{k=0}^{\infty} \int_0^{2\pi} \Phi(\psi) \exp\left[-\beta(\psi + 2k\pi)\right] d\psi = \frac{\beta}{1 - \exp\left[-2\pi\beta\right]} \int_0^{2\pi} \Phi(\psi) \exp(-\beta\psi) d\psi \tag{15}$$

and then Eq. (13) takes the form:

$$f = \frac{\beta}{1 - \exp\left[-2\pi\beta\right]} \int_0^{2\pi} n_{b1}\left(\pi V_{Tb1}^2\right)^{-3/2} \exp\left[-\xi_1^2 / V_{Tb1}^2 - \beta\psi\right] d\psi \,. \tag{16}$$

In the uniform crossed electric and magnetic fields the electron trajectory is a trochoid. In Eq. (16), the integral is calculated along a part of the phase trajectory, which corresponds to a single period of the trochoid in the coordinate space. If the plasma parameters vary little over distances of the order of the trochoid height, the integrand in Eq. (16) can be represented as the Taylor series on $(z_1 - z)$. Restricting ourselves to linear terms of the expansion, we obtain:

$$f = \frac{\beta\, n_b\left(\pi V_{Tb}^2\right)^{-3/2}}{1 - \exp\left[-2\pi\beta\right]} \int_0^{2\pi} \left\{ 1 - (z - z_1)\left[\frac{1}{n_b}\frac{dn_b}{dz} + \left(\frac{2\xi_1^2}{V_{Tb}^2} - 3 \right) \frac{1}{V_{Tb}} \frac{dV_{Tb}}{dz} \right] \right\} \exp\left(-\xi_1^2 / V_{Tb}^2 - \beta\psi\right) d\psi \,. \tag{17}$$

The coordinates difference $(z - z_1)$ and the velocity square ξ_1^2 may be expressed through the phase ψ, with the help of Eq. (12) as follows:

$$z - z_1 = \frac{c_\perp}{\omega_c}\left(\cos\chi - \cos\varphi\right), \tag{18}$$

$$\xi_1^2 = c^2 + W^2 + 2Wc_\perp \cos\chi \,, \tag{19}$$

where $\chi = \psi - \arctan\left(c_z / c_y\right)$; $c_\perp = \sqrt{c_y^2 + c_z^2}$. For convenience of the further analysis, we will use the following dimensionless variables:

$$F = f\, V_{Tb}^3 / n_b \,; \qquad \mathbf{u} = \mathbf{c}/V_{Tb} \,; \qquad \mathbf{w} = \mathbf{W}/V_{Tb} \,; \qquad \mathbf{v} = \mathbf{w} + \mathbf{u} \,; \qquad \zeta = \omega_c z / V_{Tb} \,. \tag{20}$$

After substituting Eq. (18) and Eq. (19) to Eq. (17) and changing the variables according to Eq. (20), the ultimate expression of the distribution function takes the form:

$$F = \frac{1}{\pi^{3/2}} \frac{\beta \exp\left(-w^2 - u^2\right)}{1 - \exp(-2\pi\beta)} \int_0^{2\pi} \left[1 + A_n \frac{1}{n_b}\frac{dn_b}{d\zeta} + A_T \frac{1}{T_b}\frac{dT_b}{d\zeta} \right] \exp\left(-2wu_\perp \cos\chi - \beta\psi\right) d\psi \,, \tag{21}$$

where

$A_n = u_y - u_\perp \cos\chi;$ $\qquad A_T = A_{T0} + A_{T1}\cos\chi + A_{T2}\cos 2\chi;$

$A_{T0} = u_y\left(w^2 + u^2 - \dfrac{3}{2}\right) - wu_\perp^2;$ $\qquad A_{T1} = -u_\perp\left(u^2 + w^2 - \dfrac{3}{2} - 2wu_y\right);$ $\qquad A_{T2} = -wu_\perp^2 .$

In the Hall type discharge the momentum transfer collision frequency is much smaller than the Larmor frequency, so, our interest is in the asymptotic form of the distribution function at $\beta \to 0$. In this case, we have $\beta / \left[1 - \exp(-2\pi\beta)\right] \to 1/(2\pi)$ and the dimensionless EVDF takes the form:

$$F = \frac{\exp\left(-w^2 - u^2\right)}{\pi^{3/2}}\left[I_0 + \left(u_y I_0 + u_\perp I_1\right)\frac{1}{n_b}\frac{dn_b}{d\zeta} + \left(A_{T0} I_0 - A_{T1} I_1 + A_{T2} I_2\right)\frac{1}{T_b}\frac{dT_b}{d\zeta}\right], \quad (22)$$

where $I_k\left(2wu_\perp\right) = \left(1/\pi\right)\int_0^\pi \exp\left(2wu_\perp \cos t\right)\cos(kt)\,dt$, $k = 0,1,2$ are the modified Bessel functions of the first kind. The asymptotic distribution function (22) has a particularly simple form in a homogeneous plasma:

$$F = \frac{\exp\left(-w^2 - u_x^2 - u_\perp^2\right)}{\pi^{3/2}} I_0\left(2wu_\perp\right). \quad (23)$$

This form is somewhat like the form of distribution function, called the "thermal ring"[24]

$$F_{th}^{(j)} = \frac{1}{\pi\alpha^2 j!}\left(\frac{u_\perp}{\alpha}\right)^{2j}\exp\left(-u_\perp^2/\alpha^2\right), \quad j = 0,1,2,\ldots, \quad (24)$$

which is used in studying cyclotron harmonic phenomena in magnetized plasma[25,26].

IV. Structure of the Distribution Function

In the absence of a birth temperature gradient, Eqs. (21) and (22) contain a velocity component u_x only in the factor $\exp\left(-w^2 - u^2\right) \sim \exp\left(-u_x^2\right)$. Therefore, in the direction of the magnetic field the EVDF is Maxwellian. At arbitrary values of the Hall parameter in the presence of the birth temperature gradient, the Maxwellian character of the EVDF in the direction of the magnetic field is disturbed because the coefficients A_{T0}, A_{T1} depend on a square of the velocity u^2, which includes the term u_x^2. But also in this case, the electron velocity distribution along the direction of the magnetic field remains symmetrical with respect to the velocity u_x .Therefore, in this section we will consider the EVDF in a plane perpendicular to the direction of the magnetic field, calculating it at $u_x = 0$. Also, for better clarity of the diagrams we will normalize the EVDF to its maximum value.

A. Spatially Uniform Plasma

In spatially uniform plasma, the dimensionless distribution function depends on the two parameters: $\beta = \nu/\omega_c$ and $w = W/V_{Tb} = \left(E/B\right)\sqrt{m/\left(2T_b\right)}$. The distribution function in the limit of rare collisions $\beta \to 0$ calculated with using Eq. (22) for spatially uniform plasma is exemplified in Fig. 1.

In the absence of the electric field ($w = 0$) the distribution function is Maxwellian. In the presence of the electric field, a maximum of the function becomes flatter with the increasing parameter w, and at some point, the EVDF acquires a crater shape. The reason for the formation of such a form is illustrated in Fig. 2.

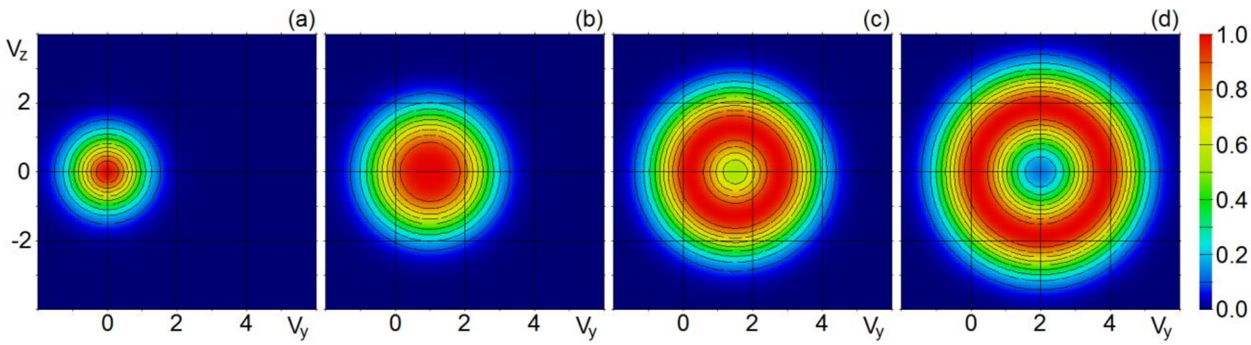

Figure 1. EVDF in the uniform plasma at $\beta \to 0$: (a) $w = 0.0$; (b) $w = 1.0$; (c) $w = 1.5$; (d) $w = 2.0$.

In the absence of the electric field ($w = 0$) the distribution function is Maxwellian. In the presence of the electric field, a maximum of the function becomes flatter with the increasing parameter w, and at some point, the EVDF acquires a crater shape. The reason for the formation of such a form is illustrated in Fig. 2.

Figure 2(a) shows in the coordinate space the electron trajectories in the shape of a trochoid that are distinguished by different initial velocities. Here and in all subsequent examples, it is believed that $B_x > 0$ and $E_z > 0$. The projections of the relevant phase trajectories on the corresponding plane in the velocity space are shown in Fig. 2 (b). On the so-called prolate trochoid, shown by a dashed line in Fig 2 (a), some of the characteristic points are numbered. On the right side of the figure, corresponding points in the velocity space are depicted.

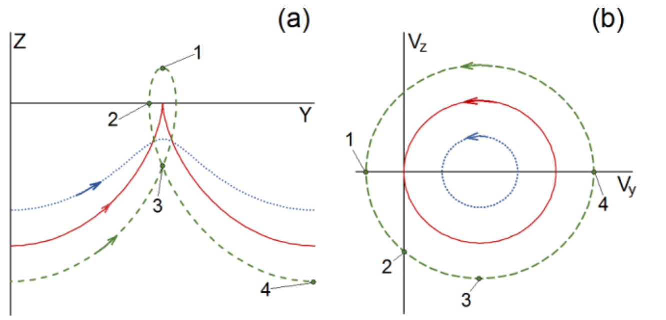

Figure 2. Projections of some typical phase trajectories of electrons on: (a) the coordinate plane, perpendicular to the magnetic field; (b) the corresponding plane in the velocity space.

A continuous line shows a cycloid, in which electrons move with the zero initial velocity after collision. In the limiting case of perfectly inelastic collisions, for example, when all the electron energy is spent on ionization and excitation, the initial velocity after the collision V_{Tb} is close to zero and we have $w >> 1$. In this case, the distribution function differs significantly from zero in a small neighborhood of the circle, which corresponds to a trajectory in the form of a cycloid shown in Figure 2 (b) with the continuous line. Therefore, the EVDF has a crater shape with narrow walls. The number of electrons moving in the prolate and curtate trajectories, shown in Figure 2 by the dashed and dotted lines, respectively, grows with the increase of the average EBDF thermal velocity V_{Tb}. In the velocity space, this leads to a broadening of the EVDF crater walls. In the limit $w \to 0$, when the average birth thermal velocity is much higher than the drift velocity, the crater walls merge, as the width of the walls becomes much greater than the distance between them and EVDF becomes close to Maxwellian.

Figures 3 and 4 show the EVDF calculated with using Eq. (21) at the finite collision rate for spatially uniform plasma at $w = 1$ and $w = 2$ respectively for several values of the parameter β.

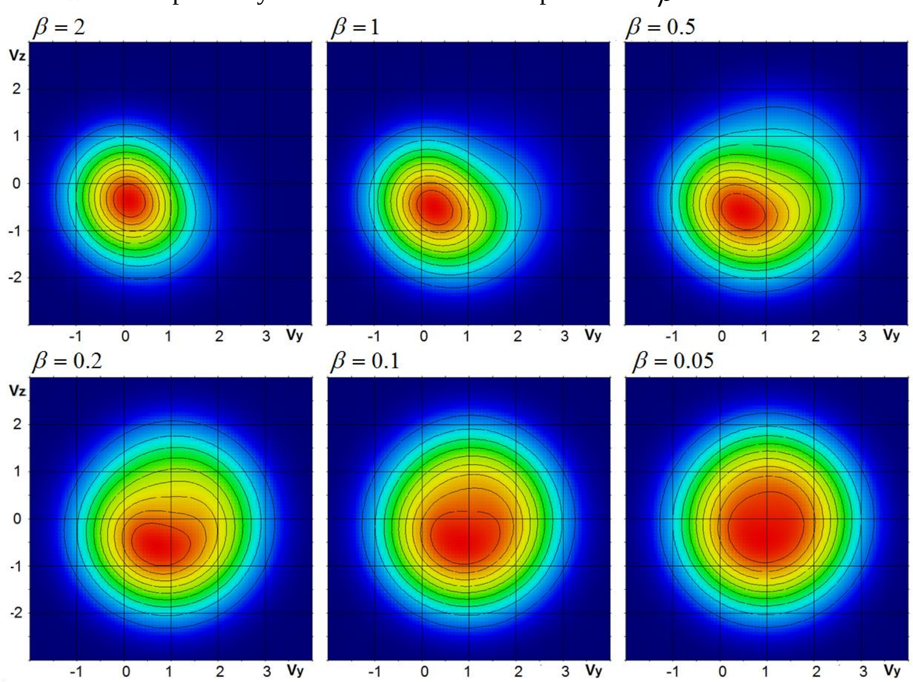

Figure 3. EVDF in the uniform plasma at $w = 1.0$ for several values of the parameter β ..

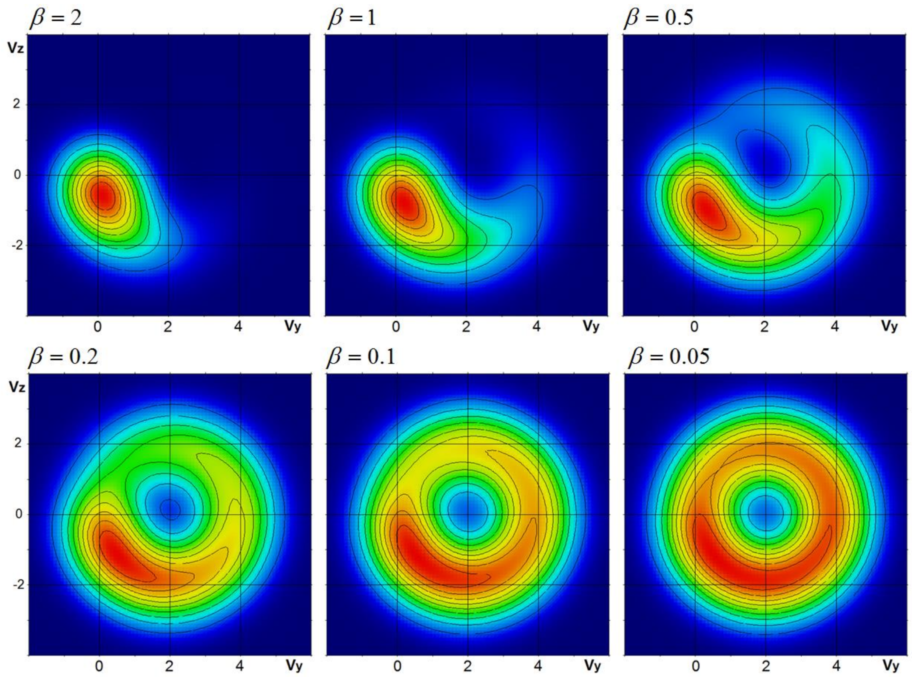

Figure 4. EVDF in the uniform plasma at $w = 2.0$ for several values of the parameter β.

At a high collision frequency, the distribution function is close to equilibrium and has a small shift of the maximum along the circumference that corresponds to a cycloid trajectory with the zero initial speed. The vector of this displacement determines the components of the drift velocity and mobility. With the decrease of the parameter β, i.e., at the reduction of the collision frequency, as compared to the Larmor frequency, the region occupied by comparatively high values of the EVDF extends along the circumference which corresponds to a cycloid trajectory. In the limit of rare collisions, the EVDFs tend to the asymptotic functions shown in Fig. 1. Thus, the asymptotic of the EVDFs shown in Fig. 3 at $\beta \to 0$ is the function shown in Fig 1(b). The asymptotic of the EVDFs shown in Fig. 4 at $\beta \to 0$ is the function shown in Fig 1(d). At this limit the drift velocity tends to the value of $W = E/B$, and the velocity component along the electric field tends to zero.

B. Plasma with Electron Number Density and Temperature Gradients

Now we consider the effect of the electron number density and temperature gradients in the direction of the electric field on the EVDF. For brevity, we will use the notations $(\ln n_b)' = (1/n_b)dn_b/d\zeta$, and $(\ln T_b)' = (1/T_b)dT_b/d\zeta$.

Figure 5 shows the examples of the EVDF in the limit of rare collisions ($\beta \to 0$) at $(\ln n_b)' = 0.1$, $(\ln T_b)' = 0$ In the absence of the electric field ($w = 0$) the EVDF is close to Maxwellian distribution and has a slight displacement in the direction v_y that corresponds to the speed of the diamagnetic drift. In the presence of the electric field, the direction of the diamagnetic drift coincides with the direction of the drift in the crossed electric and magnetic fields. The comparison of the distribution functions calculated in the absence and the presence of the electron number density gradient gives the best visual representation of distinctions between the two types of drift. Comparing the diagrams in Fig. 1. and Fig. 5, we see that the drift in the crossed $\mathbf{E}\times\mathbf{B}$-fields appears as a displacement of the crater center from the origin, and the diamagnetic drift corresponds to the skewed heights of the crater walls.

.

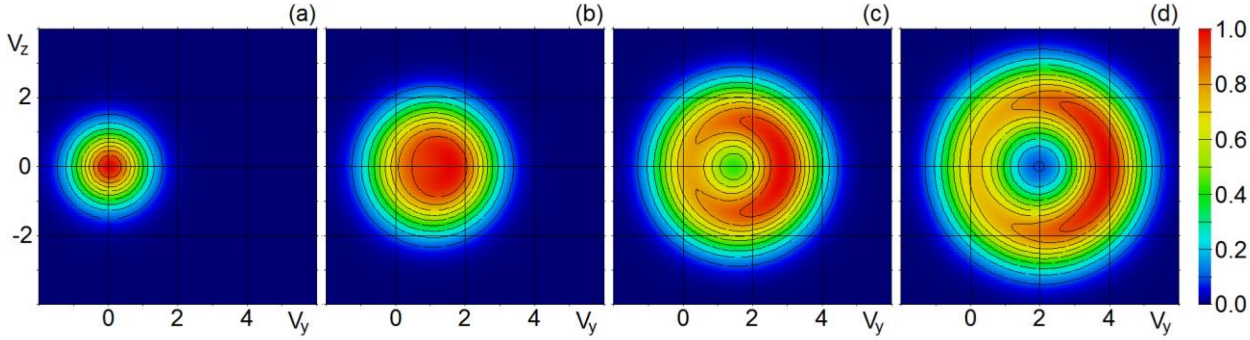

Figure 5. EVDF at $(\ln n_b)' = 0.1$**;** $(\ln T_b)' = 0$**;** $\beta \to 0$**: (a)** $w = 0.0$**; (b)** $w = 1.0$**; (c)** $w = 1.5$**; (d)** $w = 2.0$**.**

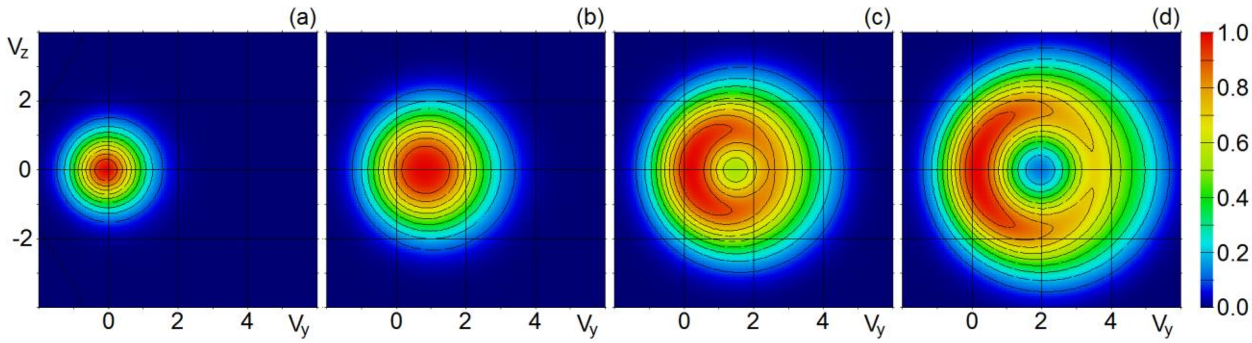

Figure 6. EVDF at $(\ln n_b)' = 0$**;** $(\ln T_b)' = 0.1$**;** $\beta \to 0$**: (a)** $w = 0.0$**; (b)** $w = 1.0$**; (c)** $w = 1.5$**; (d)** $w = 2.0$**.**

Figure 6 shows the examples of the EVDF in the limit of rare collisions ($\beta \to 0$) at $(\ln n_b)' = 0$, the temperature gradient $(\ln T_b)' = 0.1$, and $w = 0.0; 1.0; 1.5; 2.0$. An interesting feature of the distribution function in the absence of the electric field ($w = 0$) is a small shift of the maximum of the distribution function toward the region of negative values of the velocity component $\mathrm{v_y}$. At the same time, the average velocity component V_y calculated numerically for this distribution function is greater than zero, which is consistent with the classical theory.

V. Moments of the Distribution Function

Macroparameters of the obtained distribution function can be calculated analytically. The resulting integrals are reduced to the Laplace transform of functions in the form $(\sin\psi)^m(\cos\psi)^n$, where $m, n = 0,1,2,...$. Another way of calculating the moments based on the use of the saddle point approximation, in which the explicit form of the distribution function was not calculated, was described in Ref. 27. The expansions of macroparameters in terms of the powers of the $(z - z_1)$, contained the members up to the second order inclusive. Therefore, the resulting expressions of moments included the first and the second derivatives of the EBDF macroparameters. In this paper, we present the expressions obtained by direct integration of the function (21), which contain only spatial derivatives of the first order. For convenience of the comparison with classical expressions, all the macroparameters are presented in the dimensional form.

A. Electron Number Density

Integration of the function (21) over speed yields the following expression for the electron number density:

$$n = n_b + \frac{1}{\omega_c^2 + \nu^2}\frac{eE}{m}\frac{dn_b}{dz}. \tag{25}$$

If the electric field is zero, from Eq. (25) it follows, that $n_b = n$, which, according to the mass conservation law (4), corresponds to the condition $\nu_i = 0$. Since Eq. (25) corresponds to a stationary solution of the kinetic equation, we can conclude that if the electric field is zero, a stationary state is possible only in absence of ionization. If $E \neq 0$, then eliminating from Eq. (25) the number density n_b by means of Eq. (4), we get:

$$\frac{1}{n}\frac{dn}{dz} = -\frac{\nu_i\left(\omega_c^2 + \nu^2\right)}{\nu + \nu_i}\frac{m}{eE}. \tag{26}$$

Thus, from Eq. (26) it follows that in the presence of ionization collisions ($\nu_i > 0$) the steady state may be reached, if $dn/dz < 0$, i.e. with a decrease of the electron number density in the direction of the electric field.

B. Average Velocity

In the case of an arbitrary value of the Hall parameter, the expressions of the macroparameters are very cumbersome[27]. Therefore, in the following we consider the case of high Hall parameters, which is typical for magnetrons and Hall type plasma sources. In this limit, the average velocity components in the plane perpendicular to the magnetic field, expressed in terms of the EBDF parameters, have the form:

$$V_y = W + \left(T_b + \frac{1}{2}mW^2\right)\frac{1}{m\omega_c n_b}\frac{dn_b}{dz} + \frac{1}{m\omega_c}\frac{dT_b}{dz}. \tag{27}$$

$$V_z = -\beta\left[W + \left(T_b - \frac{1}{4}mW^2\right)\frac{1}{m\omega_c n_b}\frac{dn_b}{dz} + \frac{1}{\omega_c m}\frac{dT_b}{dz}\right]. \tag{28}$$

The velocity component V_x equals zero, since the EVDF is symmetrical with respect to the velocity ξ_x. Substituting the EBDF parameters from Eqs. (4) and (5) into Eq. (28) and neglecting the convective derivatives dV_y/dz and dV_z/dz, we get the following expression for the diffusion rate in the direction of the electric field:

$$V_z = -\frac{(\nu + \nu_i)}{\omega_c^2}\frac{eE}{m} - \frac{\nu}{\omega_c^2}\frac{1}{mn}\left[(1 - \Delta_c + \Delta_V)T\frac{dn}{dz} + n\frac{dT}{dz}\right], \tag{29}$$

where $\Delta_c = \dfrac{\nu_x\langle\varepsilon_x\rangle}{\nu\varepsilon_T} + \dfrac{\nu_i\varepsilon_i}{\nu\varepsilon_T}$; $\Delta_V = \left(\dfrac{13\nu + 9\nu_i}{4\nu}\right)\dfrac{\varepsilon_D}{\varepsilon_T}$.

For convenience of the results interpretation, we introduced here the characteristic energy of the thermal motion $\varepsilon_T = 3T/2$ and the characteristic drift energy $\varepsilon_D = mW^2/2$.

Comparing this expression with Eq. (10), we see that the hydrodynamic and kinetic approaches provide the same magnitude of the electron mobility caused by the electric field. In both cases the effective collision frequency, which determines the mobility, is equal to the sum $(\nu + \nu_i)$, i.e. it includes the doubled frequency of ionization collision. In case $dn/dz = 0$, the expressions of the diffusion rate caused by the temperature gradient in hydrodynamic and kinetic approximations also have a similar form. The diffusion rate caused by the electron number density gradient contains an adjustment Δ_c that takes into account inelastic collisions, as well as the kinetic correction Δ_V due to the non-Maxwellian nature of the distribution function. It has been revealed above, that for $w << 1$, i.e. when the energy of the directed drift velocity is much smaller, than the thermal energy ($\varepsilon_D << \varepsilon_T$), the EVDF tends to the Maxwell function. In the case $\Delta_V \to 0$ and in the absence of inelastic collisions, Eq. (29) becomes the classical expression of the diffusion rate.

C. Stress Tensor and Temperature

The asymptotic values of the stress tensor components expressed in terms of the EBDF parameters at the high Hall parameters are of the form:

$$P_{ij} = \delta_{ij} n_b T_b + \alpha_{ij} n_b m W^2 + \left(\eta_{ij} \frac{T_b}{\omega_c} + \gamma_{ij} \frac{mW^2}{\omega_c} \right) W \frac{dn_b}{dz} + \eta_{ij} \frac{n_b}{\omega_c} W \frac{dT_b}{dz}, \tag{30}$$

where $\alpha_{yy} = \alpha_{zz} = 1/2$; $\alpha_{yz} = \beta/4$; $\gamma_{yy} = \gamma_{zz} = 1/2$; $\gamma_{yz} = 5\beta/12$; $\eta_{xx} = 1$; $\eta_{yy} = \eta_{zz} = 2$; $\eta_{yz} = \beta/2$, and the remaining coefficients equal zero.

These expressions explain the occurrence of kinetic correction to the diffusion rate caused by the pressure gradient. According to Eq. (9), the diffusion rate in the hydrodynamic approximation is proportional to the sum of the two gradients: $\beta(dP_{zz}/dz)$ and dP_{yz}/dz. In this sum, the contribution of the off-diagonal component dP_{yz}/dz is usually neglected. Using Eq. (30) and considering only the first- order derivatives, we obtain the following expressions of these two terms:

$$\beta(dP_{zz}/dz) = \beta(T_b + mW^2/2)(dn_b/dz) + \beta n_b (dT_b/dz), \tag{31}$$

$$dP_{yz}/dz = (\beta/4) m W^2 (dn_b/dz). \tag{32}$$

We see, that the contribution of the P_{zz} and P_{yz} gradients to the diffusion rate are of the same order of smallness in the parameter $\beta = \nu/\omega_c$. Therefore, a neglect of the off-diagonal component of the stress tensor under certain conditions may be incorrect. Since the derivative dP_{yz}/dz contains no temperature gradient, the component P_{yz} does not influence on the thermal diffusion rate. As we have seen above, at the uniform electron number density, the thermal diffusion rate obtained in the kinetic approximation coincides with the classical expression of hydrodynamics.

In the presence of the electron density gradient the contribution of P_{yz} to the diffusion rate may be neglected, if $mW^2 << T_b$, i.e. when $\varepsilon_D << \varepsilon_T$. As shown above, this case corresponds to the EVDF, which is close to the Maxwellian one. If the drift energy $mW^2/2$ is comparable with the EBDF temperature T_b, the neglect of the off-diagonal component of the stress tensor is incorrect. In this case, the EVDF differs appreciably from the Maxwellian, and, according to Eq. (29), the kinetic corrections to the drift velocity become significant.

For the arbitrary Hall parameter all the three temperatures T_x, T_y and T_z differ from each other[20, 27]. In the limit of very rare collisions the EVDF is symmetrical with respect to the velocity $\xi_y = W$, and is characterized by two different temperatures: $T_x = T_b$ and $T_\perp = T_y = T_z = T_b + mW^2/2$. Thus, the longitudinal and transverse temperatures differ in the considered approximation by the value of the characteristic electron drift energy. We pay attention to this, since in the current hybrid models the electron temperature is usually considered isotropic.

The steady-state solution (21) establishes a certain relation between the frequencies of elastic and inelastic collisions and the gradient of the mean temperature $T = (T_x + T_y + T_z)/3$. For example, at $\beta \to 0$ in the absence of ionization collisions, from Eq. (4) and Eq. (25) it follows condition $dn_b/dz = 0$ and from Eq. (30) we obtain:

$$T = T_b + \frac{mW^2}{3} + \frac{5}{3} \frac{W}{\omega_c} \frac{dT}{dz}, \tag{33}$$

which after the substitution to Eq. (5) gives the following condition for keeping the steady state:

$$\frac{7}{2}\frac{W}{\omega_c}\frac{dT}{dz} = -mW^2 + \frac{\nu_x}{\nu_m}\langle\varepsilon_x\rangle, \tag{34}$$

The presence of a temperature gradient is explained as follows. In crossed electric and magnetic fields after the collisions, electrons acquire the velocity of directional drift that during subsequent collisions with slow heavy atoms is converted into thermal velocity. Thus, at a distance of the Larmor radius, the electrons acquire thermal energy corresponding to the traversed potential difference. This leads to the appearance of a temperature gradient, unless there are inelastic collisions that compensate for this growth.

D. Heat Flux

The components of the heat flux vector in the plane perpendicular to the magnetic field, expressed in terms of the EBDF parameters at $\beta^2 << 1$ have the form:

$$q_y = -\frac{mW^4}{4\omega_c}\frac{dn_b}{dz} + \left(\frac{mW^2}{2} + T_b\right)\frac{5n_b}{2m\omega_c}\frac{dT_b}{dz}, \tag{35}$$

$$q_z = \beta\left[n_b\frac{mW^3}{2} + \left(\frac{mW^2}{6} + T_b\right)\frac{3W^2}{2\omega_c}\frac{dn_b}{dz} + \left(\frac{17}{20}mW^2 - T_b\right)\frac{5n_b}{2m\omega_c}\frac{dT_b}{dz}\right], \tag{36}$$

Substituting here the EBDF parameters from Eqs. (4), (5), we obtain the following expressions for the components of the heat flux vector:

$$q_y = \frac{\nu_i}{\nu}\frac{nmW^3}{4} + \left(1 - \Delta_c + \Delta_{q1}\right)\frac{5nT}{2m\omega_c}\frac{dT}{dz}, \tag{37}$$

$$q_z = -\left(1 - \Delta_c - \Delta_{q2}\right)\frac{\nu\nu_i}{\nu+\nu_i}\frac{3nWT}{2\omega_c} - \left(1 - \Delta_c - \Delta_{q3}\right)\frac{\nu^2}{\nu+\nu_i}\frac{5nT}{2m\omega_c^2}\frac{dT}{dz}, \tag{38}$$

where $\Delta_{q1} = \left(\frac{5\nu + 3\nu_i}{2\nu}\right)\frac{\varepsilon_D}{\varepsilon_T}$, $\quad \Delta_{q2} = \frac{2\nu^2 + \nu\nu_i + \nu_i^2}{2\nu\nu_i}\frac{\varepsilon_D}{\varepsilon_T}$, $\quad \Delta_{q3} = \left(\frac{31\nu + 51\nu_i}{20\nu}\right)\frac{\varepsilon_D}{\varepsilon_T}$.

Both components of the heat flux consist of the two terms. The first terms describe the heat flux due to ionization collisions. This part of the flow is not related to the temperature gradient, but is due to the electron drift. Note, that in the current hybrid models, the heat flux is usually neglected or assumed to be proportional to the temperature gradient like in the near-equilibrium flows. The second terms in Eqs. (37) and (38) are due to the temperature gradient. We have seen above that the presence of ionization collisions in the steady state is possible only with a non-zero gradient of the electron density. Therefore, both terms, in fact, arise due to the pressure gradient.

The same correction Δ_c, as in Eq. (29) accounts for the presence of inelastic collisions. The corrections Δ_{q1}, Δ_{q2}, and Δ_{q3} result from nonequilibrium of the EVDF. These corrections tend to zero at $\varepsilon_D/\varepsilon_T \to 0$, i.e., when the EVDF tends to the Maxwellian distribution. The second term in Eq. (38) describes the thermal conductivity in the direction of the temperature gradient. In the limit $\varepsilon_D/\varepsilon_T \to 0$ and in the absence of ionization collisions, this expression coincides with the classical expression for the heat flux[23]

$$q_z = -\nu\frac{5nT}{2m\omega_c^2}\frac{dT}{dz}, \tag{39}$$

The second term in Eq. (37) describes the Ettingshausen effect[28], i.e. the heat transfer in the direction perpendicular to the temperature gradient.

VI. Numerical Study of the Electrostatic Electron Cyclotron Instability

A. Motivation

A practical application of the corrections to the transport coefficients due to the nonequilibrium character of the obtained distribution function is restricted by the accepted conditions of the stationary state and absence of the plasma gradients along the drift velocity. The narrow range of the applicability of the obtained results is directly related to the impossibility of a strict hydrodynamic description of the electron flow characterized by large Hall parameters. In order that hydrodynamic description be true, one or another process in plasma should result in the establishment of some universal EVDF that is characterized by several integral magnitudes. It is important thereat, that this distribution would established in a time substantially lesser than the characteristic time of large-scale non-stationary processes, and at distances that are considerably smaller than the characteristic dimensions of the flow heterogeneity. In classical hydrodynamics, the closeness of the distribution function to equilibrium is maintained by frequent collisions with the short mean free path. In the Hall discharge the collisions are rare, and as we have seen a rapid cyclotron rotation does not ensure the similarity of the resulting distribution functions.

However, collisions are not the only process, as a result of which the EVDF can acquire some universal form at a short time and at short distances. In principle, such a process can consist in development of small-scale high frequency electrostatic kinetic instability. In the magnetized plasma with Maxwellian EVDF the electrostatic waves pertain to stable oscillations[29]. However, in several studies it has been shown that the electrostatic electron cyclotron instability involving Bernstein modes may arise due to a delta function ring or thermal ring electron distribution[30-34]. The form of the distribution function with the shape of the crater, obtained in the present paper, is close to the form of the thermal ring. Therefore, it was interesting to study the stability of the obtained EVDF and to trace the evolution of this function if the instability does occur. If in the process of the instability development the EVDF is modified to some universal form, a promising task is to find this form and calculate the corresponding expressions for the tensors of viscosity and thermal conductivity. In this case, a prospect of the justified use of the hydrodynamic approach to the electron flow description in the Hall type discharge may open.

We are planning systematical study of the instability for the most common EVDF given by Eq. (21) as a direction of the future work. To check whether there is a high frequency electrostatic instability at all for a given type of the distribution function in this study we are investigating the stability of the asymptotic function (23) that corresponds to a homogeneous plasma in the limit of very rare collisions.

B. Dispersion Relation

The EVDF given by Eq. (23) after integration over speed u_x and returning to the dimensional variables takes the form

$$f\left(c_\perp\right)=\frac{n}{V_{Tb}^2}\exp\left(-\frac{c_\perp^2+W^2}{V_{Tb}^2}\right)I_0\left(\frac{2c_\perp W}{V_{Tb}^2}\right). \tag{40}$$

This function depends only on the relative velocity module $c_\perp$. The general dispersion relation for Bernstein modes propagating perpendicular to the magnetic field in homogeneous and collisionless plasma for the case when the distribution function depends only on the velocity modulus is given by[35]

$$k^2=\frac{2\pi e^2}{\varepsilon_0 m}\int_0^\infty dc_\perp\frac{\partial f_0}{\partial c_\perp}\left[1-J_0^2\left(\frac{|k|c_\perp}{\omega_c}\right)-\sum_{j=1}^{\infty}\frac{2\omega^2}{\omega^2-\left(j\omega_c\right)^2}J_j^2\left(\frac{kc_\perp}{\omega_c}\right)\right], \tag{41}$$

where J_j is the Bessel function of the first kind of order j.

We numerically solved the dispersion relation (41) with EVDF given by Eq. (40) for four values of the ratio $w=W/V_{Tb}=2,3,4,5$. The plasma to cyclotron frequency ratio $\omega_p/\omega_c=\sqrt{ne^2/\varepsilon_0 m}/(eB/m)$ was set to 10 which is typical value for the Hall type discharge. Figure 7 shows the dispersion curves obtained. The real frequency (black) and growth rate (blue) normalized to cyclotron frequency ω_c are plotted versus normalized wave number kW/ω_c.

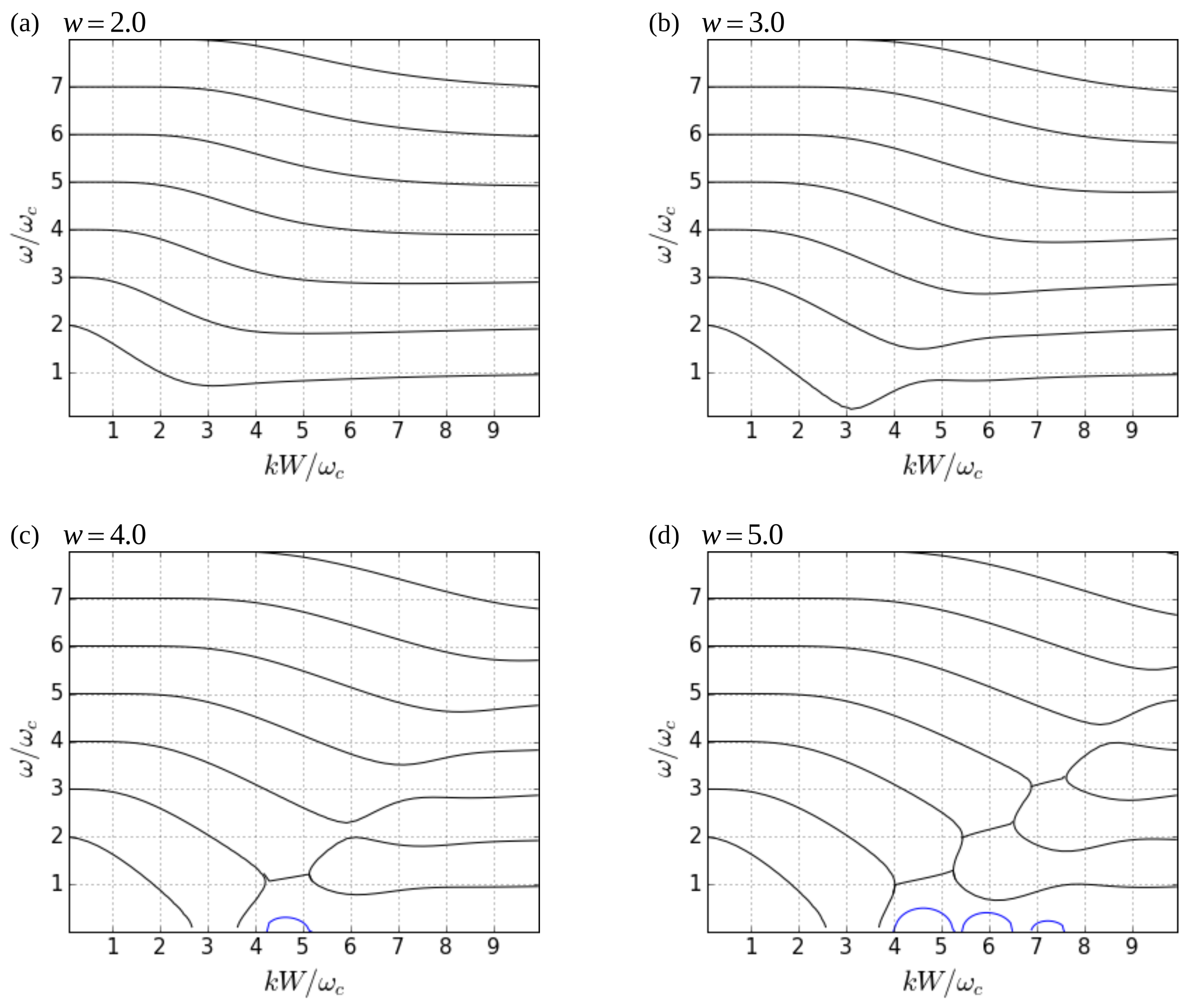

Figure 7. The normalized real frequency (black) and growth rate (blue) for Bernstein waves plotted versus normalized wave number keeping $(\omega_p/\omega_c) = 10$ and varying $w = W/V_{Tb}$: (a) $w = 2.0$; (b) $w = 3.0$; (c) $w = 4.0$; (d) $w = 5.0$.

At relatively high thermal spread ($w = 2, 3$) the roots of the dispersion relation are real and waves are stable like the classic Bernstein modes with Maxwellian transverse velocity distribution. As the thermal spread is reduced ($w = 4, 5$) the imaginary parts of the roots appear and solutions become absolutely unstable. It means that the waves will grow in time to amplitudes limited only by the validity of the small-signal theory which has been used in obtaining the dispersion relation (41). The imaginary frequency components in the considered cases are very strong. Indeed, when the parameter w is equal to 4, the imaginary component of (ω/ω_c) reaches ~0.3 which corresponds to the growth rates of ~16 dB per cyclotron period.

To study the nonlinear saturation of the wave electric field and the EVDF evolution in time during the development of instability we developed a 1D2V (one space and two velocity dimensions) particle-in-cell simulation code.

C. Numerical Model and Simulation Results

As in the previous considerations we choose an orthogonal coordinate system in which the uniform magnetic field B and the uniform electric field E are directed along the *x*-axis and *z*-axis, respectively. The spatial variation of the electron space charge and perturbation of the electric field is in the *y* direction. The ions are immobile and constitute a uniform charge neutralizing background. The electron collisions are neglected because we are interested in the electrostatic high frequency oscillations at short time period which is much less than the mean free time between collisions. In absence of the collisions the electron velocity along the magnetic field is constant and therefore we excluded the *x*-component of the velocity from consideration. Acceleration by the Lorentz force was integrated using the 4-step Boris method. Particle position was computed using the Leapfrog method. The potential variation is obtained by integrating the Poisson equation. On the ends of the space domain with length L the periodical boundary conditions were specified.

Electrons were loaded in such a way to provide sinusoidal distribution $n = n_0(1+\gamma \sin(ky))$ in the space and the distribution given by Eq. (23) in velocity space. Here $k = 2\pi/L$ is a wave number. The undisturbed electron number density n_0 was equal to the ion background number density. The disturbance factor γ was adjusted in such a way to provide the initial amplitude of the wave electric field component $E_y = 10^{-2} E_T$, where $E_T = \sqrt{n_0 T/\varepsilon_0}$ is the characteristic thermal electric field. The number of cells was set to provide the cell size not higher than $0.5\lambda_D$. One period of the electron plasma oscillations was resolved by approximately 50 time steps and the total simulation time reaches 6 cyclotron periods. Simulation consisted of $5 \cdot 10^6$ particles. The simulations were performed at a domain length corresponding to the wave number $k = 4.5(\omega_c/W)$. The plasma to cyclotron frequency ratio (ω_p/ω_c) was set to 10. A series of calculations was performed for the EFDV (23) with $w = 1, 2, 3, 4, 5, 6$.

Figures 8 and 9 show the results of simulations. On each element of the figures, in the bottom the evolution of the normalized wave energy in time is shown. The time in the wave energy diagram is expressed in units of the cyclotron rotation period $(\omega_c t)/(2\pi)$. The normalized wave electric field energy was calculated as the ratio of the wave electric field energy ε_E to its value at the initial time ε_{E0}. In the top of each element of the figures four diagrams with the distribution function calculated in the middle of the space domain at the times moments corresponding to 0, 2, 4, and 6 of the cyclotron periods are shown. In order not to clutter the drawing, we did not show in the EVDF diagrams the axes and the color scales. On the parameters of the electron velocity axes, one can get a representation based on Figures 1-6. All distribution functions are normalized on the maximum value and the color scale corresponds to the scale shown in Fig. 1.

As can be seen from Figs. 8-9, the results of numerical simulation are consistent with the conclusions obtained from the analysis of the dispersion relation. At $w = 3$ and less, the wave is stable, and at $w = 4$ and higher instability develops.

In all the analyzed regimes, the Landau damping occurs in the initial period of time. Then the attenuation ceases and the wave passes to the stationary oscillation regime.

At $w = 3$ and less the stationary undamped oscillations continue unchanged for many cyclotron periods. The form of the EVDF does not change appreciably in this case, retaining the form like a flattened Gaussian distribution ($w = 1$) or the shape of the crater ($w = 2, 3$).

At $w = 4$ and higher after the initial damping, the wave energy begins to increase and, even during the first period of cyclotron rotation, begins to exceed the energy of the initial perturbation. Then the energy of the wave increases and within one or two cyclotron periods reaches nonlinear saturation. The initial annular form of the distribution function begins to deform and approximately after 4-6 cyclotron periods, the EVDF acquires a complex fuzzy shape.

The calculations show that both the total energy and the total entropy of the system remain constant within the limits of the accuracy of the calculations and the error associated with numerical heating. For all the presented results, the energy conservation law is performed with relative accuracy up to 10^{-4}. Thus, when an instability occurs, the distribution function does not tend to an equilibrium distribution. In this case the EVDF is isentropically transformed to some other kind, the properties of which can be the subject of further research.

Another direction for future research will be analysis of the instability for distribution functions, taking into account the electron number density and temperature gradients. The skewing of the walls of the crater for these functions can become a factor that significantly influences the development of instability.

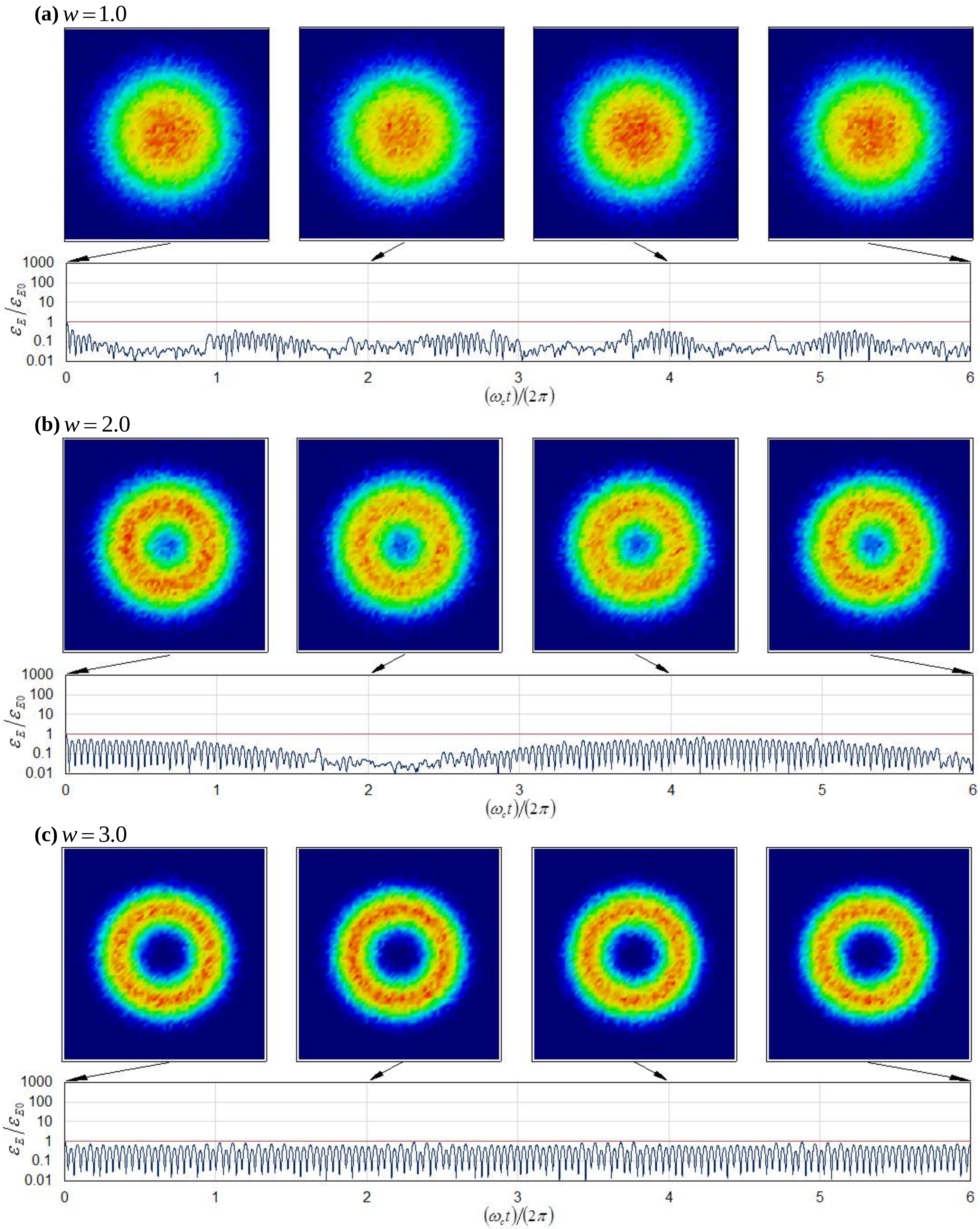

Figure 8. The evolution of the normalized wave energy in time and the EVDF diagrams at specified time moments (more explanation in the text): (a) $w = 1.0$; (b) $w = 2.0$; (c) $w = 3.0$.

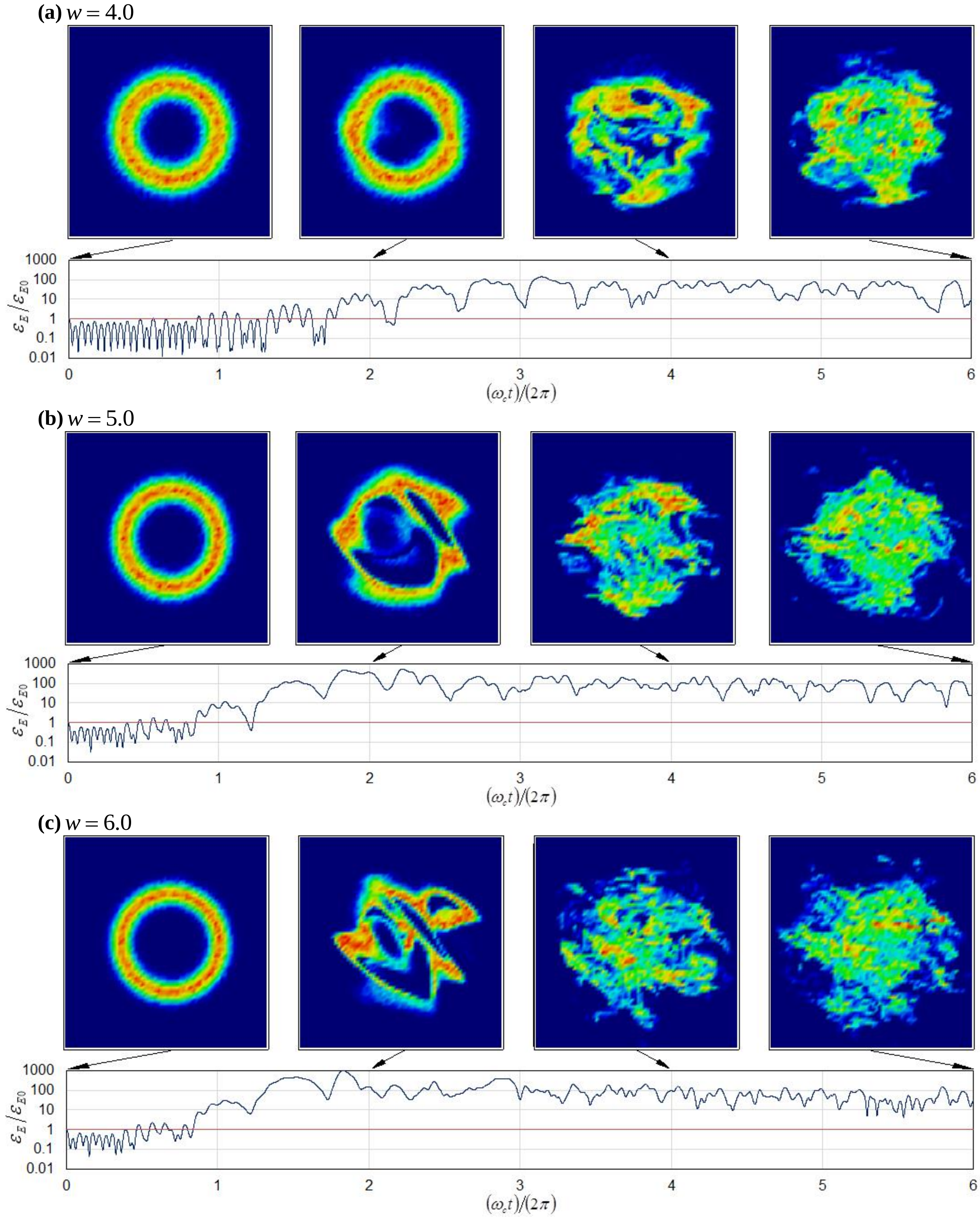

Figure 9. The same as Fig. 8 for: (a) $w = 4.0$ **; (b)** $w = 5.0$**; (c)** $w = 6.0$**.**

VII. Conclusion

A new analytical kind of the nonequilibrium electron velocity distribution function in a non-uniform weakly ionized Lorentz plasma with the crossed electric and magnetic fields has been derived as a solution of the model kinetic equation in the stationary approximation. The solution has the integral form for arbitrary values of the Hall parameter. In the limit of large Hall parameters typical for the Hall type discharge, the solution comes down to the product of the Maxwell function into a combination of the modified Bessel functions of the first kind.

The moments of the distribution function, including components of the average velocity, the stress tensor, and the heat flux have been calculated for the case of small electron momentum transfer collision frequency compared with Larmor frequency. It has been revealed, that the kinetic corrections to the rate of diffusion across the magnetic field become significant when the characteristic drift velocity in the crossed fields is comparable with the characteristic thermal velocity of the electrons. From the hydrodynamic point of view, the significance of these corrections results from the fact that the pressure gradient and the gradient of the off-diagonal component of the stress tensor are comparable quantities of the same order of smallness relative to the inverted Hall parameter.

The electron temperature in the Hall discharge is anisotropic even in the approximation of a homogeneous stationary plasma and in the absence of secondary electron emission from the discharge channel walls. The temperature has three different components at a nonzero effective collision frequency and two different components in the limit when the collision frequency tends to zero. At high Hall parameter, the temperature components in the plane perpendicular to the magnetic field is higher than the temperature in the direction of the magnetic field by the characteristic value of the electron drift energy.

In the presence of ionization collisions, the heat flux vector has components that are due to the electron drift and are not related to the temperature gradient. In the limiting case, when the electron thermal velocity is much higher than the drift velocity, the obtained distribution function tends to Maxwellian, and its transport characteristics, including mobility, diffusion and heat conduction coincide with the known expressions of the classical theory.

A preliminary investigation of the high frequency electrostatic instability due to the electron velocity distribution obtained for a homogeneous plasma in the limit of very rare collisions has been carried out. The analysis of the dispersion relation at the electron plasma to cyclotron frequency ratio $\omega_p / \omega_c = 10$ which is typical for the Hall type discharge showed the existence of stationary undamped oscillations at relatively high thermal spread, i.e. when the drift velocity to the birth thermal velocity ratio ($w = W / V_{Tb}$) is 3 or less. As the thermal spread is reduced ($w = 4, 5$) the solutions become unstable. If the instability arises, then the distribution function is isentropically transformed to the other kind with complex shape. If the instability does not arise, the form of the distribution function is retained at long characteristic hydrodynamic scales of time.

References

[1]Zhurin, V. V., Kaufman, H. R., and Robinson, R. S., “Physics of closed drift thrusters,” *Plasma sources science and technology*, Vol. 8, 1999, pp. R1-R20.

[2]Morozov, A. I. and Savelyev, V. V., “Fundamentals of Stationary Plasma Thruster Theory,” in book: *Reviews of Plasma Physics Theory*, New York, Kluver,Vol. 21, 2000, pp. 203-391.

[3]Boyd, I. D., “Simulation of electric propulsion thrusters,” Nato Report RTOEN-AVT-194, paper 17 (University of Michigan, Ann Arbor, Michigan, USA, 2011).

[4]Komurasaki, K., and Arakawa, Y., “Two-Dimensional Numerical Model of Plasma Flow in a Hall Thruster,” *Journal of Propulsion and Power*, Vol. 11, No. 6, 1995, pp. 1317-1323.

[5]Fife, J. M., "Hybrid-PIC Modeling and Electrostatic Probe Survey of Hall Thrusters," Ph.D. Thesis, Aeronautics and Astronautics, Massachusetts Institute of Technology, 1998.

[6]Hagelaar, G. J. M., Bareilles, J., Garrigues, L., and Bouef, J. P., "Role of Anomalous Electron Transport in a Stationary Plasma Thruster Simulation," *Journal of Applied Physics*, Vol. 93, No. 1, 2003, pp. 67-75.

[7]Koo, J. W., Boyd, I. D., "Modeling of anomalous electron mobility in Hall thrusters," *Physics of Plasmas*, Vol. 13, No. 3, March 2006.

[8]Parra, F. I., Ahedo, E., Fife, J. M., and Martinez-Sanchez, M., "A Two-Dimensional Hybrid Model of the Hall Thruster Discharge," *Journal of Applied Physics*, Vol. 100, 2006, p. 023304.

[9]Hagelaar, G. J. M., “Modelling electron transport in magnetized low-temperature discharge plasmas,” *Plasma Sources Science and Technology*, Vol. 16, No. 1, 2007, p. S57.

[10]Mikellides, I. G., and Katz, I., “Numerical simulations of Hall-effect plasma accelerators on a magnetic-field-aligned mesh”, *Physical Review E*, Vol. 86, 2012, p. 046703.

[11]Hara, K., and Boyd, I.D., “Low Frequency Oscillation Analysis of a Hall Thruster Using a One-Dimensional Hybrid-Direct Kinetic Simulation,” *33rd International Electric Propulsion Conference*, Washington, 2013, Paper IEPC-2013-266.

[12]Shimura, N., and Makabe, T., "Electron velocity distribution function in a gas in E×B fields," *Applied Physics Letters*, Vol. 62, 1993, pp. 678-680.

[13]Zhang, F., Ding, Y., Li, H. Wu, X., and Yu, D., "Effect of anisotropy of electron velocity distribution function on dynamic characteristics of sheath in Hall thrusters," *Physics of Plasmas*, Vol. 18, 2011, p. 103512.

[14]Balescu, R., *Transport Processes in Plasmas. Classical Transport Theory*, Elsevier Science, Amsterdam, 1988, Vol. 1.

[15] Kotelnikov, I.A., "Braginskii and Balescu kinetic coefficients for electrons in Lorentzian plasma," *Plasma Physics Reports*, Vol. 38, 2012, pp. 608-619.

[16]Meezan, N.B., and Cappelly, M.A., "Electron Energy Distribution Function in a Hall Discharge Plasma", *37th Joint Propulsion Conference and Exhibit*, Salt Lake City, 2001, Paper AIAA-2001-3326.

[17]Bugrova, A. I., Lipatov, A. S., "Energy distribution function of electrons in a low-temperature plasma in external E and H fields close to a scattering wall," *High Temperature*, Vol. 22, 1984, pp. 1–5.

[18]Kaganovich, I. D., Raitses, Y., Sydorenko, D., and Smolyakov, A., "Kinetic effects in a Hall thruster discharge," *Physics of Plasmas*, Vol. 14, 2007, p. 057104.

[19]Sydorenko, D., Smolyakov, A., Kaganovich, I. D., and Raitses, Y., "Effects of non-Maxwellian electron velocity distribution function on two-stream instability in low-pressure discharges," *Physics of Plasmas*, V. 14, 2007, p. 013508.

[20]Shagayda, A., "Stationary electron velocity distribution function in crossed electric and magnetic fields with collisions," *Physics of Plasmas,* V. 19, 2012, p. 083503.

[21]Choueiri, E. Y., "Plasma oscillations in Hall thrusters," *Physics of Plasmas,* Vol. 8, 2001, p. 1411.

[22]Bhatnagar, P. L., Gross, E. P., and Krook, M., "A model for collision processes in gases. Small amplitude process in charged and neutral one-component systems," *Physical Review*, Vol. 94, 1954, pp. 511-525.

[23]Kogan, M. N., *Rarefied Gas Dynamics*, Plenum Press, New York, 1969.

[24]Dory, R.A., Guest, G. E., and Harris, E. G. "Unstable electrostatic plasma waves propagating perpendicular to a magnetic field," *Physical Review Letters*, Vol. 14, 1965, pp. 131-133.

[25]Zheleznyakov, V.V., and Zlotnik, E. Ya., "Cyclotron wave instability in the corona and origin of solar radio emission with fine structure. I. Bernstein modes and plasma waves in a hybrid band," *Solar Physics,* Vol. 43, 1975, pp. 431–451.

[26]Grach, S. M., "On kinetic effects in the ionospheric F-region modified by powerful radio waves," *Radiophysics and Quantum Electronics*, Vol. 42, 1999, pp. 572–588.

[27]Shagayda, A.A., Stepin, S.A., and Tarasov, A.G., "Electron velocity distribution moments for collisional inhomogeneous plasma in crossed electric and magnetic fields," *Russian Journal of Mathematical Physics*, Vol. 22, 2015, pp. 532-545.

[28]Chapman A.G., and Cowling, T., *The Mathematical Theory of Non-Uniform Gases*, Cambridge University Press, Cambridge, UK, 1939.

[29]Bernstein, I. B., "Waves in a Plasma in a Magnetic Field," *Physical Review*, Vol. 109, 1958, p. 10.

[30]Crawford, F. W., and Tataronis, J. A., "Absolute Instabilities of Perpendicularly Propagating Cyclotron Harmonic Waves," *Journal of Applied Physics*, Vol. 36, 1965, p. 2930.

[31]Yoon, P. H., Hadi, F., and Qamar, A. "Bernstein instability driven by thermal ring distribution," *Physics of Plasmas*, Vol. 21, 2014, p. 074502.

[32]Eliasson, B., Speirs, D.D., and Daldorff, L.K.S., "Electrostatic electron cyclotron instabilities near the upper hybrid layer due to electron ring distributions," *Plasma Physics and Controlled Fusion*, Vol. 58, 2016, p. 095002.

[33]Leuterer, F., "Forward and backward Bernstein waves", *Plasma Physics*., Vol. 11, 1969, p. 615.

[34]Tataronis, J. A., Crawford, F. W., "Cyclotron harmonic wave propagation and instabilities, 2, Oblique propagation," *Journal of Plasma Physics*, Vol. 4, 1970, p. 249.

[35]Krall, N.A., and Trivelpiece, A.W., *Principles of Plasma Physics*, McGraw-Hill, New York, 1973.